



Titre: Initial wear of cutting coated tools while machining TiMMC
Title:

Auteurs: Mina Marousi, Roland Bejjani, & Marek Balazinski
Authors:

Date: 2025

Type: Article de revue / Article

Référence: Marousi, M., Bejjani, R., & Balazinski, M. (2025). Initial wear of cutting coated tools while machining TiMMC. *Wear*, 578–579, 206222 (14 pages).
Citation: <https://doi.org/10.1016/j.wear.2025.206222>

 **Document en libre accès dans PolyPublie**
Open Access document in PolyPublie

URL de PolyPublie: <https://publications.polymtl.ca/66455/>
PolyPublie URL:

Version: Version officielle de l'éditeur / Published version
Révisé par les pairs / Refereed

Conditions d'utilisation: Creative Commons Attribution-Utilisation non commerciale-Pas d'oeuvre dérivée 4.0 International / Creative Commons Attribution-NonCommercial-NoDerivatives 4.0 International (CC BY-NC-ND)
Terms of Use:

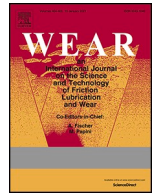
 **Document publié chez l'éditeur officiel**
Document issued by the official publisher

Titre de la revue: *Wear* (vol. 578–579)
Journal Title:

Maison d'édition: Elsevier BV
Publisher:

URL officiel: <https://doi.org/10.1016/j.wear.2025.206222>
Official URL:

Mention légale: ©2025 The Authors. Published by Elsevier B.V. This is an open access article under the CC BY-NC-ND license (<http://creativecommons.org/licenses/by-nc-nd/4.0/>).
Legal notice:



Initial wear of cutting coated tools while machining TiMMC

M. Marousi^{a,*}, R. Bejjani^b, M. Balazinski^a

^a Department of Mechanical Engineering, Polytechnique Montreal, 2900 Blvd. Edouard-Montpetit, H3T 1J4, Montreal, QC, Canada

^b Department of Mechanical Engineering, Lebanese American University, Byblos, Beirut, Lebanon

ARTICLE INFO

Keywords:

Titanium metal matrix composite
Machining
Turning
Tool wear

ABSTRACT

This research investigates the early stages of wear in PVD-coated carbide tools during the machining of titanium metal matrix composites (TiMMCs) and aims to establish a correlation between initial wear signals and eventual tool failure. A combination of direct characterization techniques including scanning electron microscopy (SEM), energy-dispersive X-ray spectroscopy (EDS), and focused ion beam (FIB) along with indirect monitoring methods such as cutting force and vibration signal analysis, was employed. Fractal analysis was applied to the recorded signals to identify wear transition points.

Initial wear manifestations, such as coating delamination, material adhesion, and microcracking, were found to progressively develop into more severe wear mechanisms like diffusion, deep cracking, and edge chipping. These wear transitions were successfully correlated with irregular signal patterns, particularly through changes in fractal dimensions. The findings demonstrate that early wear indicators can reliably predict subsequent tool failure.

By establishing a link between early-stage wear mechanisms and final failure modes, this study enhances the understanding of tool degradation in TiMMC machining. The gained insights contribute to the development of more effective wear monitoring systems, supporting increased efficiency and reliability in industrial machining operations.

1. Introduction

The machining of hard-to-cut materials, such as metal matrix composites (MMCs), remains insufficiently explored due to the non-linear nature of the process and the complex interaction between deformation and temperature fields [1–3]. Among metal matrix composites (MMCs), titanium metal matrix composites (TiMMCs) stand out due to their exceptional performance. The integration of titanium carbide (TiC) particles into a Ti-6Al-4V matrix significantly improves key properties, including stiffness, mechanical strength, wear resistance, and thermal stability. These enhanced characteristics, combined with the material's low density, have contributed to the increasing demand for TiMMCs in high-performance applications across aerospace, automotive, and defence industries [4,5].

However, the machinability of TiMMCs is hindered by severe tool wear and short tool life, often resulting in poor surface quality. The reinforced TiC particles are highly abrasive, contributing to wear through surface scratching, tool cracking, and heat generation. As difficult-to-cut materials, TiMMCs subject cutting tools to extreme

tribological and thermomechanical conditions including high friction, elevated temperatures, and chemical interactions which further accelerate tool degradation [6].

Over the years, WC-Co grade cemented carbide tools have been employed for machining superalloys due to their high fracture toughness, compressive strength, and abrasion resistance. However, even at relatively low cutting speeds, the elevated temperatures generated during machining cause a significant reduction in the hot hardness of these tools, thereby limiting their performance [7].

According to ISO 3685:1993 and ISO 8688-2:1989 [8], tool life is commonly estimated by measuring the depth of the crater or flank wear. Tool wear characteristics are commonly illustrated by plotting wear progression against cutting length or machining time, resulting in a curve typically divided into three distinct stages of wear. In the initial or primary stage of tool wear, high pressure over a narrow contact area causes rapid tool wear. After the initial wear stage, flank wear increases gradually during the steady-state phase, followed by a rapid rise during the accelerated wear stage, ultimately leading to tool failure. At the first transition point, the reported wear VB_B , is approximately 0.1 mm. The

* Corresponding author.

E-mail address: mina.marousi@polymtl.ca (M. Marousi).

<https://doi.org/10.1016/j.wear.2025.206222>

Received 13 January 2025; Received in revised form 18 June 2025; Accepted 24 June 2025

Available online 28 June 2025

0043-1648/© 2025 The Authors. Published by Elsevier B.V. This is an open access article under the CC BY-NC-ND license (<http://creativecommons.org/licenses/by-nc-nd/4.0/>).

maximum flank wear, VB_B max, is set at 0.3 mm based on cutting tests conducted in accordance with ISO 3685–1993 for both continuous and interrupted machining modes.

Research has also focused on detecting the steady-state tool wear stage during the TiMMC machining. Identifying the end of the steady-state wear phase enables timely and cost-effective replacement of cutting tools before they enter the failure zone, thereby preventing catastrophic tool failure and deterioration in machining quality [9]. In the past, conventional machining of TiMMC faced challenges such as plastic deformation, cracks, large microhardness variations, residual stresses, microstructure changes, tears, laps, and phase transformations on the tool surface [6,9,10]. Abrasion was identified as the primary wear mode in the initial wear zone because of the scratching ability of hard TiC particles dispersed throughout the MMC structure in the contact zone [11].

As a result of chemical interactions between the workpiece and the insert components, a layer of titanium oxide formed on the contact surface, leading to a reduced wear rate at higher cutting speeds. During subsequent machining, a built-up edge (BUE) and a protective layer are observed. In this context, Duong et al. [9] conducted experimental studies to clarify the effects of cutting conditions on the initial tool wear progression and overall tool life, focusing on the formation of a protective wear layer in the early stages of machining. Adhesion and diffusion were identified as the primary wear mechanisms during the initial wear stage. The duration of this initial stage ranged from 2 s to 10 s, depending on the cutting speed. For the cutting speeds selected by Duong et al. the transition times were delayed as the cutting speed increased, thereby extending the tool life [9].

Bejjani et al. [10] investigated the chip morphology and microstructure evolution within the adiabatic shear band formed during the machining of TiMMC. They used a quick stop device, transmission electron microscopy (TEM), and focused ion beam (FIB) for sample preparation. Abrasion was identified as the primary wear mode [12,13]. Kamali Zadeh et al. [14] estimated tool wear during the machining of TiMMC, characterizing the wear mechanism as abrasion. The first transition period was observed within the initial seconds of machining, with VB_B measured at approximately 0.1 mm. The second transition period was identified at the 85th second, with a cutting speed of 60 m/min [14].

Marousi et al. [15] identified abrasion, adhesion, and cracking as the most significant wear modes. The reduction in workpiece surface damage and tool wear rate was attributed to the formation of a protective layer that serves as a thermal barrier during the first transition period, marking the end of the initial wear stage and the onset of the steady-state wear region. This finding was established through a fractal analysis of the force and vibration signals during the machining of TiMMC [15].

There are two primary approaches to evaluating tool wear. Direct methods involve measuring tool wear using optical instruments to assess the wear dimensions, types of surface damage, and other relevant features. Indirect methods, whether implemented online or offline, involve acquiring and recording process parameters such as cutting force, vibration, sound, acoustic emission, temperature, and surface roughness to monitor the condition of the cutting tool during machining.

[14]. Various signal-processing techniques are also applied to enhance the reliability of the signals used to extract parameters related to the tool conditions. Typically, features extracted from a signal belong to the time, frequency, time-frequency, and statistical domains. Various methods and filters can be employed to reduce noise and enhance the level of information [16]. During machining, statistical signal processing techniques, often combined with other methods, such as neural networks, fuzzy logic, genetic algorithms, or fractal analysis, are the most commonly used after signal acquisition. Although traditional signal processing has been applied in the past, recent advanced methods have proven more effective for detecting features and monitoring the machining process.

Table 1
Operational parameters and tool geometry.

Parameter	Value (Unit)
Feed rate	0.15 mm/rev
Depth of cut	0.5 mm
Cutting speed	70 mm/min

A tool condition monitoring method that assesses the impact of tool wear is fractal analysis. Among the various methods, fractal parameters are preferred due to their sensitivity and robustness. Fractal analysis can explain the properties of signals recorded during machining, including their variations. Rimpault et al. [16] discovered that during composite machining, parameters derived from acoustic emission signal analysis are more effective than those derived from cutting force signals in estimating tool wear through fractal analysis. A study on cutting force and vibration signals during the machining of CFRP during orbital drilling of a CFRP/Ti alloy stack found that fractal parameters were suitable for identifying the different wear stages.

This study aimed to identify the transitions between wear states and their underlying mechanisms when cutting TiMMC, as well as to analyze the relationship between initial tool wear and final failure during TiMMC machining. Few researchers have investigated the detection and correlation of wear phenomena across different stages of wear. This paper introduces a novel approach for comparing the initial signs of wear to the final wear during the machining of TiMMC.

Insights from previous studies on transition times and wear mechanisms during TiMMC machining have motivated the present work to investigate the relationship between wear indicators and distinct wear states. A thorough literature review revealed that limited information is available on the machining of TiMMC and the associated tool wear.

The worn surfaces were analyzed at both microscales and macroscales using scanning electron microscopy (SEM) and FIB analysis. Additionally, fractal analysis was conducted on the cutting force and vibration signals to detect transition times. Gaining a deeper understanding of the tool wear mechanisms and their characteristics across different wear states will aid in developing effective strategies to extend tool life, improve the cutting process, and increase production efficiency by managing initial wear to control the final wear.

Given that TiMMCs are novel composites, limited information is available in the literature regarding their machinability and associated challenges.

2. Experimental setup

The TiMMC workpiece used in this study consisted of a Ti–6Al–4V matrix reinforced with a 10–12 % volume fraction of irregularly shaped titanium carbide (TiC) particles. The composite was fabricated via a powder metallurgy route. Ti–6Al–4V and TiC powders were mechanically mixed to ensure uniform distribution, followed by cold compaction. The green compact was then sintered under a vacuum atmosphere at elevated temperatures to promote solid-state diffusion and bonding. This process allowed for effective dispersion of TiC particles within the matrix.

The turning parameters are detailed in Table 1. Cutting speed, feed rate, and cut depth were chosen based on prior cutting tests and recommendations from the manufacturer.

Tool wear was evaluated using a direct offline method based on optical measurements. After machining, images of the flank face were captured using a Mitutoyo optical microscope and a Canon EOS 300D digital camera to characterize wear and surface damage.

The maximum tool wear parameter was calculated as the mean of the maximum tool wear VB_B max. Tool wear progression was measured every 0.5 s under consistent cutting conditions for up to 60 s to complete the tool wear curve and extend beyond tool failure when the cutting tool would no longer be functional. This approach was based on previous

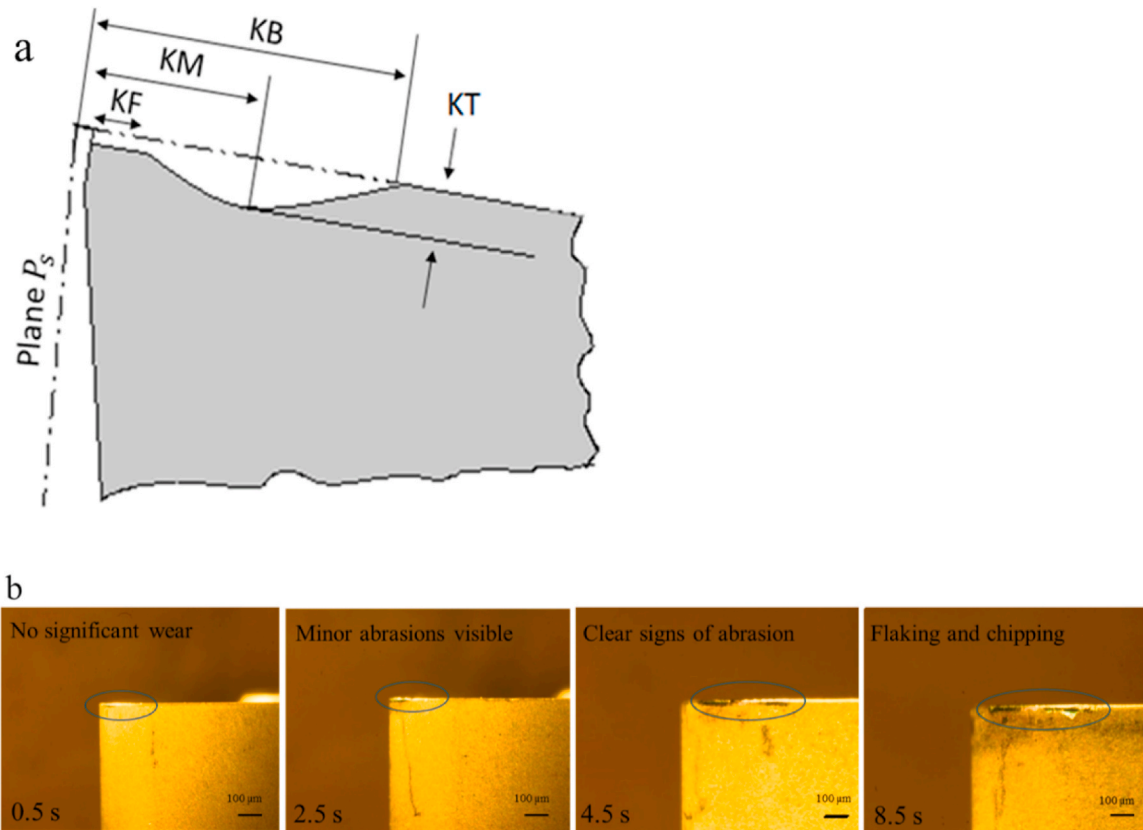


Fig. 1. (a) Flank wear land on the turning cutting edge according to the ISO 3685:1993 standard (b) Optical picture of the flank face of the insert at different cutting times while machining titanium metal matrix composite (TiMMC).

studies on turning TiMMCs using carbide tools. The optical images depicting the flank wear area on the same insert after increasing the cutting time are shown in Fig. 1.

Additionally, the tested inserts were analyzed by scanning electron microscopy (SEM), energy-dispersive X-ray spectroscopy (EDS), and focused ion beam (FIB) microscopy. These techniques were utilized to investigate the coating and assess its wear impact on its crystalline structure and texture. A JSM 7800F Aztec EDS was employed to examine the microstructure of the wear mechanism in the flank area. The JSM 7800F field emission SEM is equipped with field emission guns (FEGs), offering high resolutions of 0.8 nm at 15 kV and 1.2 nm at 1 kV, respectively, and features an Oxford EDS detector. Before imaging, the smearing material was etched away using Kroll's reagent (2 ml HF, 25 ml HNO₃, 50 ml H₂O) for at least 5 min.

All machining tests were repeated four times under identical cutting conditions to ensure data repeatability and avoid experimental artifacts. The average cutting forces was later used in the fractal analysis. Cutting force values across all trials demonstrated high consistency, with a mean value of 126.75N and a standard deviation of approximately ± 2.00 N. The force values reported here correspond to the machining time from the first moment of machining to 60 s and were used as input for the fractal dimension analysis.

Since this study is focusing on initial wear, a value of $VB = 75 \mu\text{m}$ was set as a reference point marking the transition from the initial wear phase to the steady-state region. This value was also used as a set point for correlating wear with force signal changes. The measured average value of flank wear ranged between $72 \mu\text{m}$ and $76 \mu\text{m}$, with a mean value of $74.25 \mu\text{m}$ and a standard deviation of $\pm 1.71 \mu\text{m}$.

This study focused on the details of wear on the flank face during TiMMC machining and the progression of wear. The flank face of the cutting tool was characterized at various cutting times before the initial wear (defined as 0.1 mm according to the ISO standard and previous

studies) [9,14,15]. After measuring and analyzing the flank face of the cutting tool, machining was continued until tool failure and final wear (measured at 0.3 mm).

Given the importance of verifying tool wear during the transition between different wear stages, an indirect monitoring method was employed. The amplitudes of the vibration, acoustic, and force components were measured in three directions using an accelerometer and a dynamometer mounted on the cutting tool holder. Cutting forces and vibration signals were collected during the machining process using a Kistler dynamometer (Type 9121) with a sensitivity of 500 N/V in three directions, along with a PCB Piezotronics triaxial accelerometer. The obtained signals were transmitted through an amplifier, digitized using an A/D converter at a frequency rate of 48 MHz, and recorded using a data acquisition system. Fractal analysis was then conducted to determine tool wear transition times through indirect signal processing. The accelerometer and dynamometer on the cutting tool holder measured vibration and force amplitudes in three directions. Variations in the cutting conditions, which may indicate changes in the tool conditions, resulted in system vibrations. Signal processing was employed to reduce noise, segment the data, and extract relevant information from the raw signals. Regularization analysis was selected for this study because of its robustness than other fractal methods like box counting. The fractal dimension was used to examine signal irregularities and roughness during the machining of TiMMC.

2.1. Tool material

A tungsten carbide turning insert with a PVD-coated TiN/TiAlN multilayer (CNMG 432-MF4 TS2000) was used as the cutting tool. The TS2000 series is known for its extended tool life and cost-effectiveness and is widely used for turning superalloys. This grade offers several advantages, including high productivity, excellent abrasion resistance,

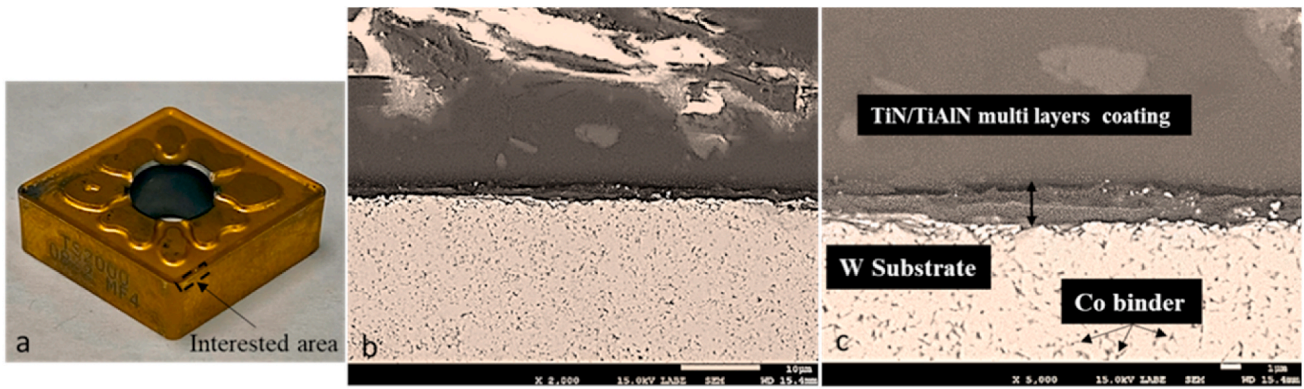


Fig. 2. (a) Optical image of the CNMG 432-MF4 TS2000 turning insert. (b) SEM image of the PVD-coated flank face. (c) Cross-sectional SEM showing the multilayer TiN/TiAlN coating, tungsten carbide (W) substrate, and cobalt (Co) binder phase.

Table 2
Properties of TiMMC and Ti-6Al-4V [17].

Property	TiMMC	Ti-6Al-4V
Yield Strength (MPa)	1014	862
Tensile Strength (MPa)	1082	965
Elastic Modulus (GPa)	135	116
Fracture Toughness (MPa√m)	40	80
Shear Modulus (GPa)	51.7	44
Hardness (HV)	~700 HV	~350–380 HV

chemical stability of the coating layers, superior surface finish, and consistent machining performance [4].

SEM analysis was performed on a new carbide insert with a PVD multilayer TiAlN/TiN coating. Fig. 2 presents the surface morphology and microstructural features of the coating, offering detailed insights into its crystallization and structural characteristics.

2.2. Workpiece material

The physical properties of TiMMC, which are superior to those of the Ti-6Al-4V alloy used as the base, are listed in Table 2. The chemical

Table 3
Chemical composition and physical and mechanical properties of TiMMC [17].

Al (Aluminum)	V (Vanadium)	C (Carbon)	O (Oxygen)	Fe (Iron)	N (Nitrogen)	H (Hydrogen)	Ti (Titanium)	Total
5.55	3.84	0.97	0.26	0.004	0.21	<0.003	Remainder (89.163)	100

composition, as well as the physical and mechanical properties of TiMMC, are also detailed in Tables 2 and 3 [13].

Fig. 3 illustrates the microstructure of the TiMMC workpiece at two different magnifications, where TiC reinforcement particles appear as dark regions embedded within the Ti-6Al-4V matrix. The TiC particles are heterogeneously distributed, with clear evidence of clustering and local agglomeration. This non-uniformity is attributed to the powder metallurgy-based manufacturing process, during which particle aggregation can occur in the mixing or sintering stages [17–20]. Quantitative image analysis of SEM micrographs (n = 100) revealed that the TiC particles had an average size of $4.2 \pm 1.3 \mu\text{m}$, with a standard deviation of approximately $1.23 \mu\text{m}$. The TiC particles exhibited predominantly irregular and angular morphologies, with a non-uniform distribution throughout the matrix. Such microstructural heterogeneity significantly influences the local mechanical response during machining, as the intermittent interaction between the cutting tool and high-hardness TiC clusters promotes localized stress concentrations and accelerates tool wear [17–20].

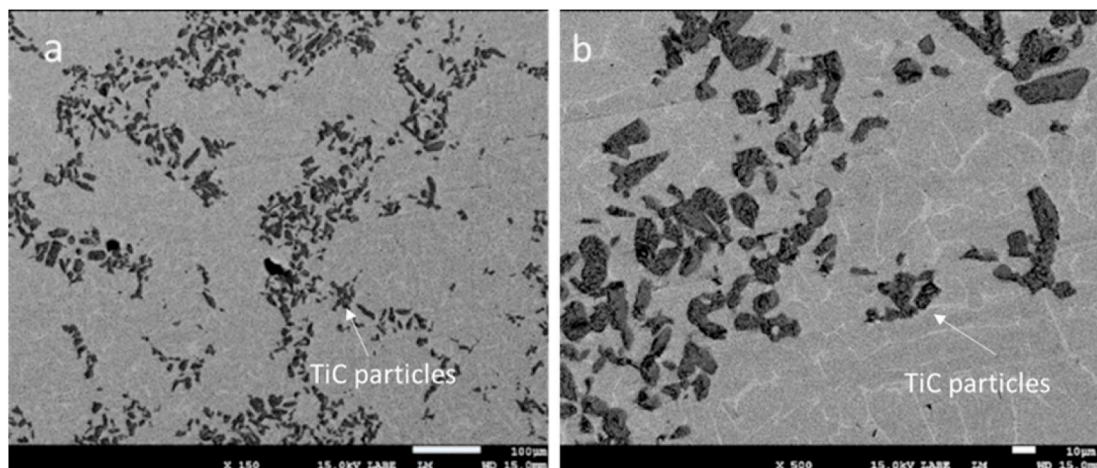


Fig. 3. (a) SEM image at $150 \times$ showing TiC particles dispersed in the matrix. (b) SEM image at $500 \times$ revealing clustered TiC particles in the TiMMC microstructure.

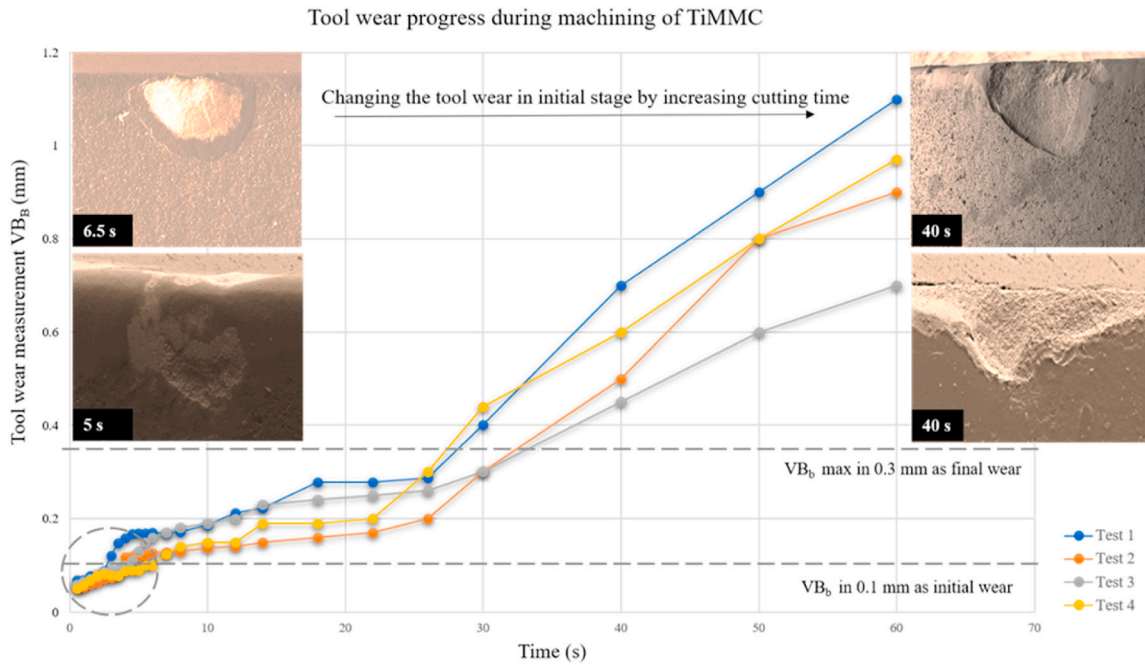


Fig. 4. Tool wear progression (VB_B) within 60 s of TiMMC machining. Examples of initial wear on the left and the resulting final wear on the right side of graph.

3. Experimental results

3.1. Tool life span

Since this study focused on initial tool wear and its relationship to final wear during TiMMC machining, the first step involved measuring the progression of flank wear (VB_B) using the cutting data provided above. The image processing results are presented in Fig. 4. The initial step involved photographing each cutting edge, followed by processing the images using the ImageJ software to measure flank wear. All VB_B measurements were then plotted on a graph. The tool life was determined to be approximately 60 s based on the tool life criterion of

VB_B max at 0.3 mm.

The cutting process using the same insert was extended to 60 s to exceed the point of tool failure, rendering the tool non-functional. This approach was guided by preliminary findings from a prior study on turning TiMMC with carbide tools.

3.2. Prediction of tool wear transitions

Signal processing can serve as a valuable tool for detecting the transition times between wear stages. Variations in cutting conditions induce corresponding vibrations within the system, enabling the assessment of tool condition through vibration and force signals. To

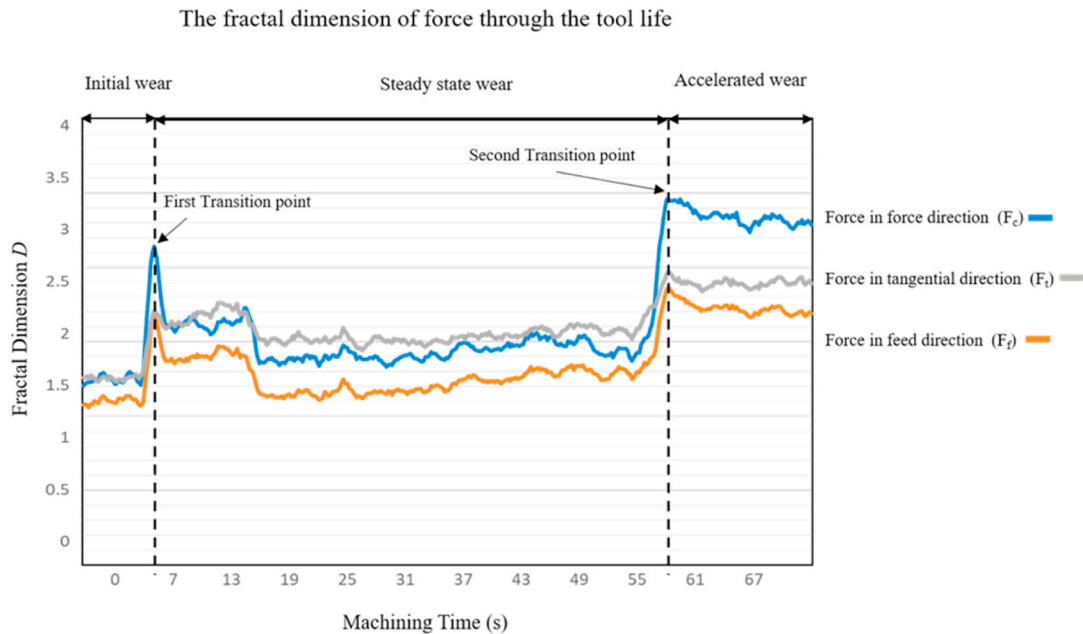


Fig. 5. The fractal parameter (fractal dimension D) versus the machining time presents the signal roughness at the transition times, which appears as a peak in the vibration and force signals.

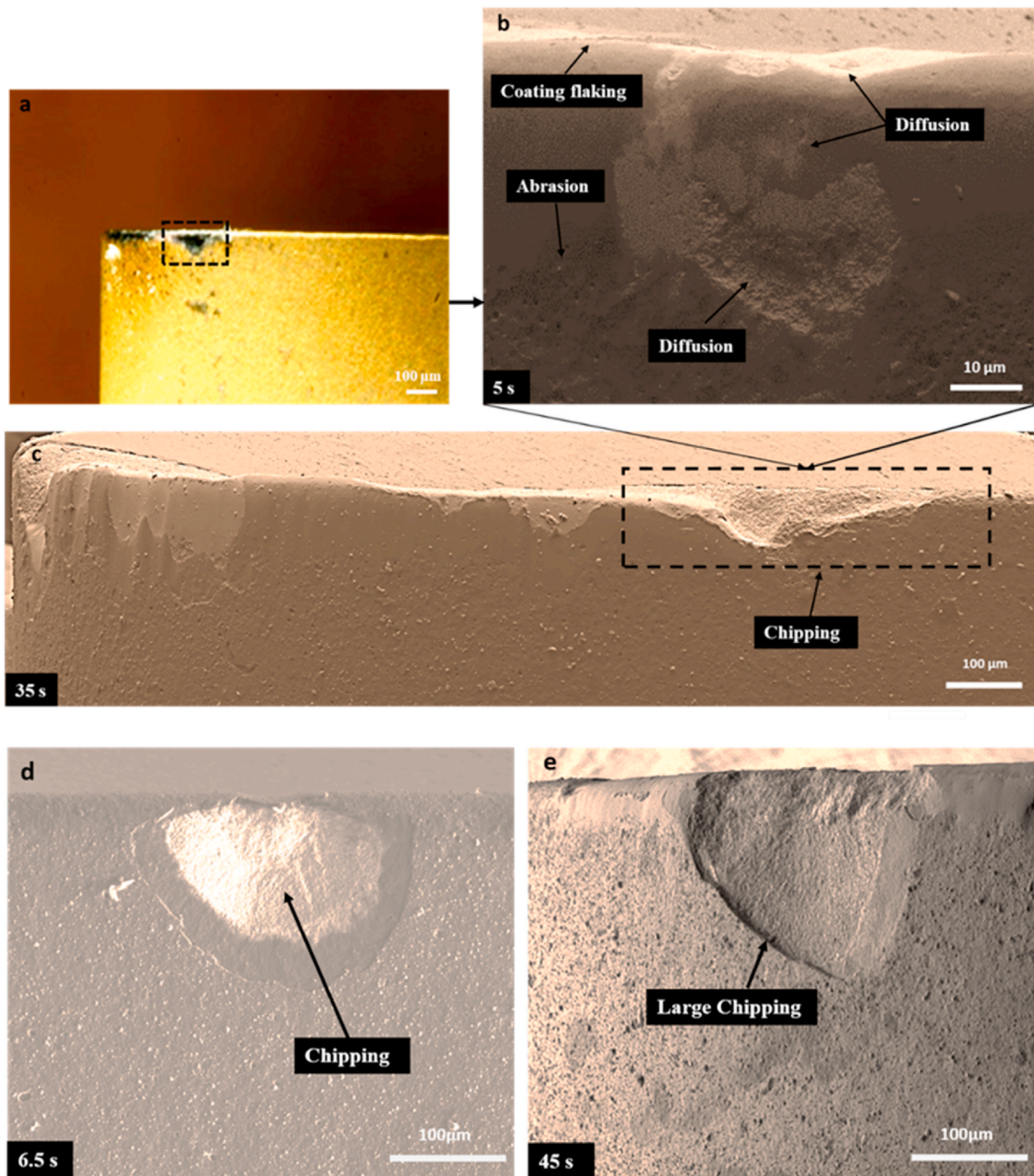


Fig. 6. (a) Selected area for wear analysis. (b) Flank face after 5 s of machining. (c) Wear progression at 35 s. (d) New insert after 6.5 s. (e) Final wear zone after 45 s of machining.

analyze these signals, researchers have employed various techniques, including fast Fourier transform (FFT), wavelet transform, and fractal analysis. However, traditional signal-processing methods are often inadequate for accurately detecting transition times. Consequently, online signal processing based on fractal analysis has been adopted to more effectively evaluate tool wear transition times.

Probability statistics theory may not provide sufficient accuracy for studying tool wear when the evolution process exhibits chaotic characteristics. Chaos theory addresses this unpredictability in a system and employs fractal parameters to predict changes in the signal shape. Fractal analysis has proven to be an efficient decision-making technique that requires minimal processing time and expertise. This method is used

to extract information from various signals for tool condition monitoring.

Based on previous work [15] an investigation using fractal analysis was made. As illustrated in Fig. 5, the transition times are indicated by the peaks in the vibration and force signals, which were analyzed using fractal analysis to extract the fractal dimension index. The transition times are shown as changes in signal roughness. **Transition points** in a tool wear graph represent key moments in the wear progression of a cutting tool during machining. These points mark shifts in the wear behavior and indicate changes in the dominant wear mechanisms or tool performance. In summary, the transition points signify the tool's journey through wear phases and highlight the need for monitoring or

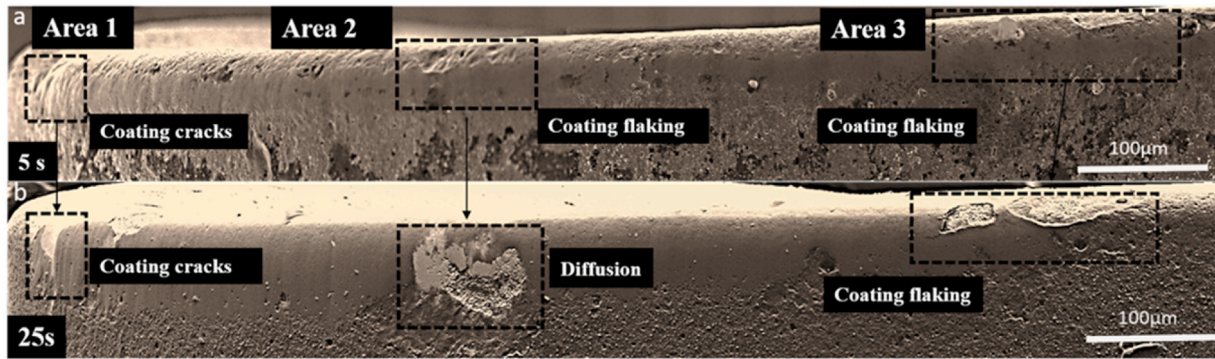


Fig. 7. SEM images of tool flank wear after (a) 5 s and (b) 25 s of machining, showing progression from initial coating cracks and flaking to diffusion damage and severe delamination.

intervention to maintain efficient and high-quality machining [15].

3.3. Wear phenomena during TiMMC turning

The micrographs of the tool were captured on the worn flank face during the turning of the TiMMC. To comprehensively document the changes in the microstructure of flank tool wear, each cutting edge was used as a unique cutting trail. The flank faces were then evaluated by elemental and chemical mapping using SEM and EDS analyses.

This study focused on the details of wear on the flank face during the initial seconds of machining TiMMC and as wear progressed. The cutting tool was characterized at various cutting times and was selected based on previous studies and preliminary testing. After analysing the flank face in the initial seconds, each cutting edge was machined until the failure wear zone was reached.

The wear mechanism during the machining of TiMMC was identified as a combination of abrasion, scratching, grooving, smearing, and cracking on the flank face. It is widely recognized that abrasion wear arises from the scratching effects of hard TiC particles dispersed throughout the structure of MMCs in the contact zone. From the initial moments of machining, various wear mechanisms can be observed. As the machining progresses, chemical wear becomes prominent, leading to the formation of an oxide layer via a chemical reaction between the insert components and the workpiece, as discussed in the next section. Additionally, other research [19] has indicated that high stresses and temperatures during machining can lead to the formation of a protective tribo-layer that serves as a protective layer on worn surfaces.

Fig. 6a, b, and c illustrate the evolution of wear on the flank face of the cutting tool from 5 s to 35 s during the machining of TiMMC. At 5 s, there are visible signs of coating flaking and material dispersion on the tool. Coating flaking indicates that parts of the protective coating layer are detached early in the coating process. Abrasion is evident as mechanical wear due to friction between the tool and the workpiece, whereas diffusion indicates material transfer and chemical interactions on the surface of the tool, likely resulting from high temperatures. By 35 s, tool wear had progressed significantly, with evident chipping observed on the flank face. The early signs of diffusion detected at 5 s likely contributed to progressive material weakening, ultimately leading to substantial chipping. This sequence illustrates how initial wear mechanisms such as coating flaking and diffusion progressively develop into more severe forms of material degradation, including chipping, as machining continues. Specifically, the wear observed at 5 s, which primarily involved diffusion and minor coating damage, advances to severe wear marked by significant chipping at 35 s. This change underscores the cumulative and progressive nature of wear during extended machining operations. Additionally, at 6.5 s (Fig. 6d), evidence of chipping is observed on the tool, indicating the onset of localized material removal from the cutting edge. This chipping indicates that the surface of the tool has begun to degrade under the mechanical and

thermal stresses experienced during machining. As shown in Fig. 6e damage intensified by 15 s, leading to a large chipping zone that further exacerbated the wear.

Fig. 7 provides additional insights into the wear progression on the flank face of the insert at various cutting times, as captured by SEM. The results also illustrate the correlation between the first signs of wear during the initial wear stage and the final wear observed when machining TiMMC with the same insert. The initial signs of wear shown in Fig. 7a indicated a transition in the type of wear observed in the final area. At the fifth second of machining, the first signs of peeling of the coating appeared on different areas as it shown in Fig. 7a. When the machining time was increased to 25 s, the abrasion and coating flaking intensified or transitioned into diffusion wear (Fig. 7b).

The different areas of interest at the fifth second of machining and after extending the machining time to 25 s with the same insert are shown in Fig. 7 b, where the flank face is divided into three distinct areas. In the initial wear state shown in Fig. 7a, detected around the 5 s mark using fractal analysis, the first layer of coating flaked and peeled off rapidly. As the coating kept wearing away, flaking became more visible, and small cracks started to form and grow into larger cracks in the worn area. Moreover, abrasion by hard particles led to the formation of grooves, as observed in Area 1. Extending the machining time to 25 s with the same insert revealed increased wear across multiple zones compared to the initial stage. In Area 1, early microcracking was observed, which subsequently led to abrasion. In Areas 2 and 3, grooves and surface adhesion appeared due to progressive coating flaking.

Diffusion was observed on the surface of the cutting tool in the flaked region of area 2 s after increasing the machining time to 25 s. In area 3, substrate removal was observed in the flaked region, indicating a cohesive flaking. The wear process began at 5 s and was characterized by coating microcracking. This exposed the substrate, leading to direct contact with the workpiece and resulting in diffusion. This weakened area eventually caused significant chipping at 25 s. Additionally, with another insert at 3.5 s (Fig. 8), the flank face exhibited a substantial build-up of adhered material, leading to a build-up edge (BUE) on the cutting edge. These observations suggest that different wear mechanisms were present at the beginning of the machining process. In the same areas, the adhered material acted as a protective layer on the worn surface and helped slow down further wear. The heat resistance of this layer likely acts as a barrier against additional wear.

The progression from initial to final wear followed a consistent pattern. The observed sequence began with the first signs of wear in the initial wear zone and developed as follows: (a) adhesion and edge flaking, (b) spontaneous and cohesive flaking of the coating, (c) adhesion to the exposed substrate, (d) diffusion, (e) cracking, and (f) severe chipping. At 2.5 s, signs of wear appeared as microcracking in the coating on the edge of the cutting tool. After an additional 1 s of machining, the wear area was observed again at 3.5 s. Fig. 8 (at 3.5 s) shows increased adhered material and signs of cohesive flaking. These

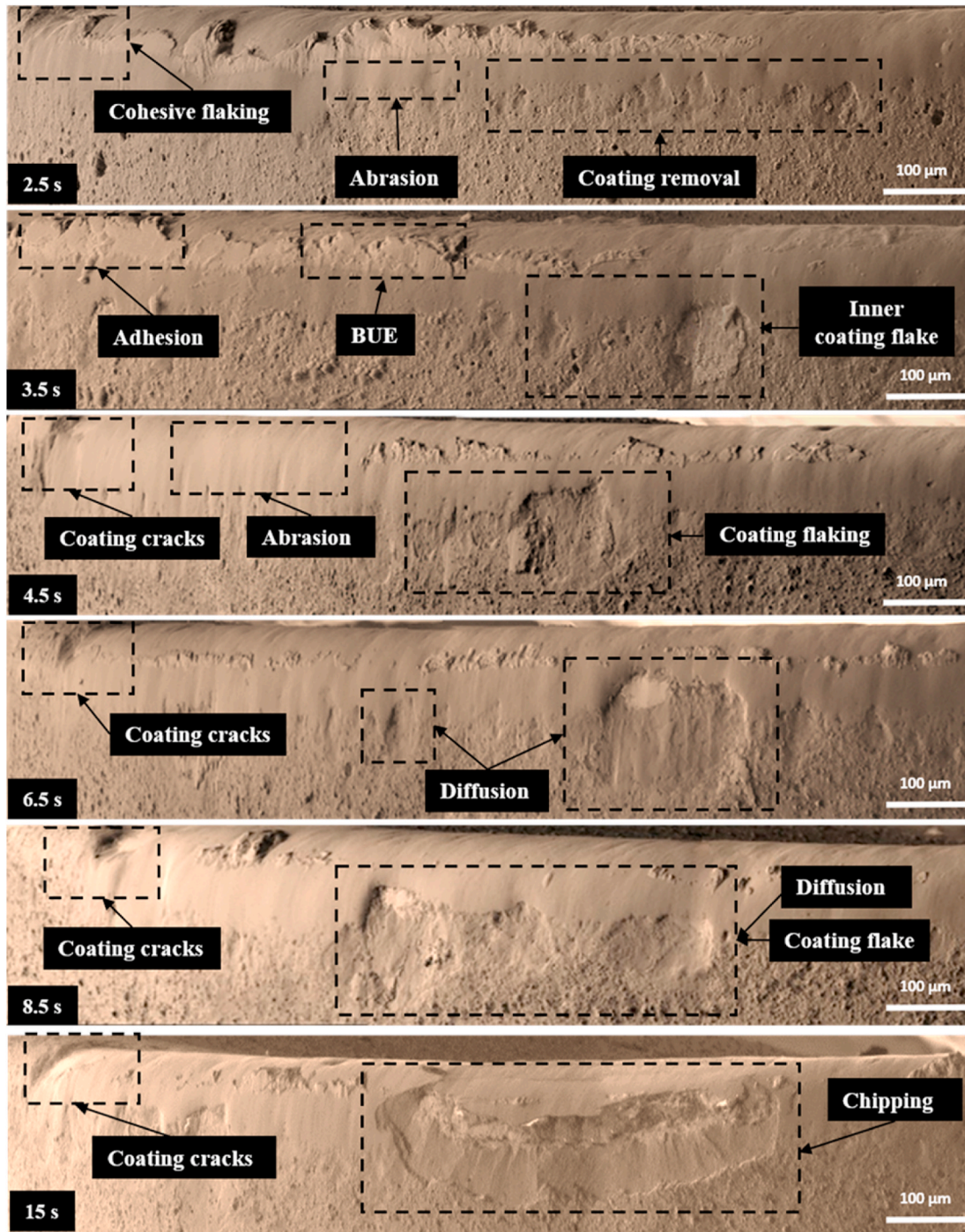


Fig. 8. SEM micrograph of the flank face at different cutting times.

changes could be linked to a higher initial wear rate. This early wear may be further exacerbated by spontaneous flaking of PVD (Physical Vapor Deposition) coatings, a phenomenon driven by high residual stress within the coating material [20,21].

Residual stress can be induced during deposition due to variations in temperature, coating thickness, and material properties, leading to internal stress buildup. When this residual stress exceeds the adhesion strength between the coating and substrate, the coating may begin to delaminate or flake off spontaneously. This degradation can significantly impair the performance and longevity of the coated tool because the protective layer designed to enhance wear resistance and reduce friction is compromised. To address this issue, careful control of the

deposition parameters and post-deposition treatments is necessary to minimize residual stress and enhance coating adhesion [22].

At 4.5 s, abrasion and crack growth were observed on the flank face. It has been reported that carbon diffusion from the tool to the workpiece, followed by the interaction of Ti atoms with carbon to form a TiC protective layer, accelerates the wear process [23].

After coating flaking, the first signs of diffusion appeared in the same area at 6.5 s. As machining progressed, the wear progressed into chipping when the cutting time reached 15 s. Table 4 details the correlation between the initial signs of wear and the final wear during the machining of TiMMC. The adhesion wear observed earlier progressed into more severe forms, including cohesive flaking and increased

Table 4
Wear evolution vs. time from initial wear signs to final wear signs.

	Initial Wear	Progressive Wear
Wear evolution ↓	BUE (Adhesion)	Edge Flaking Wear
	Adhesion	Cohesive flaking
	Spontaneous Flaking of Coating	Adhesion to Substrate
	Adhesion to Substrate	Diffusion Wear
	Diffusion Wear	Deep Cracking
	Cracks	Chipping
	Time →	

abrasion, demonstrating the progressive nature of tool wear under these conditions.

Moreover, the diffusion of elements such as carbon (C) and cobalt (Co) from the tool body to the surface can also contribute to wear. During the initial few seconds of machining, EDS analysis revealed changes in the elemental concentration, as shown in Fig. 9a. It has been reported that when the Ti1-xAlxN coatings are heated and exposed to air at extreme temperatures [24], a high concentration of Al K series elements is detected between 4.5 s and 15 s in the worn zone, corresponding to the TiAlN coating layer. Aluminium can react with oxygen in the atmosphere to form a tribofilm that serves as a protective layer [25]. Due to its thermal stability, this oxide layer can serve as a barrier, inhibiting further material degradation. However, no increase in the oxygen concentration was observed, so the formation of the Al oxide layer could not be confirmed [25].

The spectrum in Fig. 9b shows that the outer layer of the coated insert was worn away within 4.5 s of machining, leading to a change in the element concentration. Compressive stresses within the oxide layers

can lead to peeling, exposing unoxidized material and making it more susceptible to further oxidation [26]. Scratches and grooves were likely formed on the flank face of the tool due to the TiC particles being pulled from the workpiece and dragged across the surface of the tool.

3.4. FIB investigations

This study focused on the details of wear on the flank face during the machining of TiMMC, from the first few seconds until the end of the tool's life. Wear progression was characterized using SEM analyses. Further investigations at the micro and nanoscales were conducted using FIB.

FIB studies were conducted to gain insights into the relationship between the workpiece materials and the resulting worn surfaces. The additional information obtained from the worn surfaces and FIB investigations contribute to a deeper understanding of the wear mechanisms when machining TiMMC. This examination allows the analysis of coating changes and the embedding of workpiece material on the surface of the tool, facilitating the study of wear on the crystalline structure of the coating. In the initial step of FIB sample preparation, the workpiece was manually ground and then polished automatically. Subsequently, the sample was positioned in the FIB to identify the target region. The FIB enables precise local removal or deposition of the material.

FIB analysis revealed the lamella layers extracted from the worn flank, displaying the layers prepared using the FIB in situ lift-out technique. A direct correlation was observed between the cross-section and the coating surface of the specimen. The region from which the FIB layer was prepared is illustrated in Fig. 10.

As shown in Fig. 11, traces of cobalt (Co) were detected on the surface after a few seconds of machining. The detection of cobalt (Co) at the surface layer indicates that diffusion has occurred toward this region, consistent with its role as a binder phase in the substrate of the cutting tool. In the elemental mapping spectrum shown in Fig. 11, the brighter areas indicate a higher concentration of the element at a specific

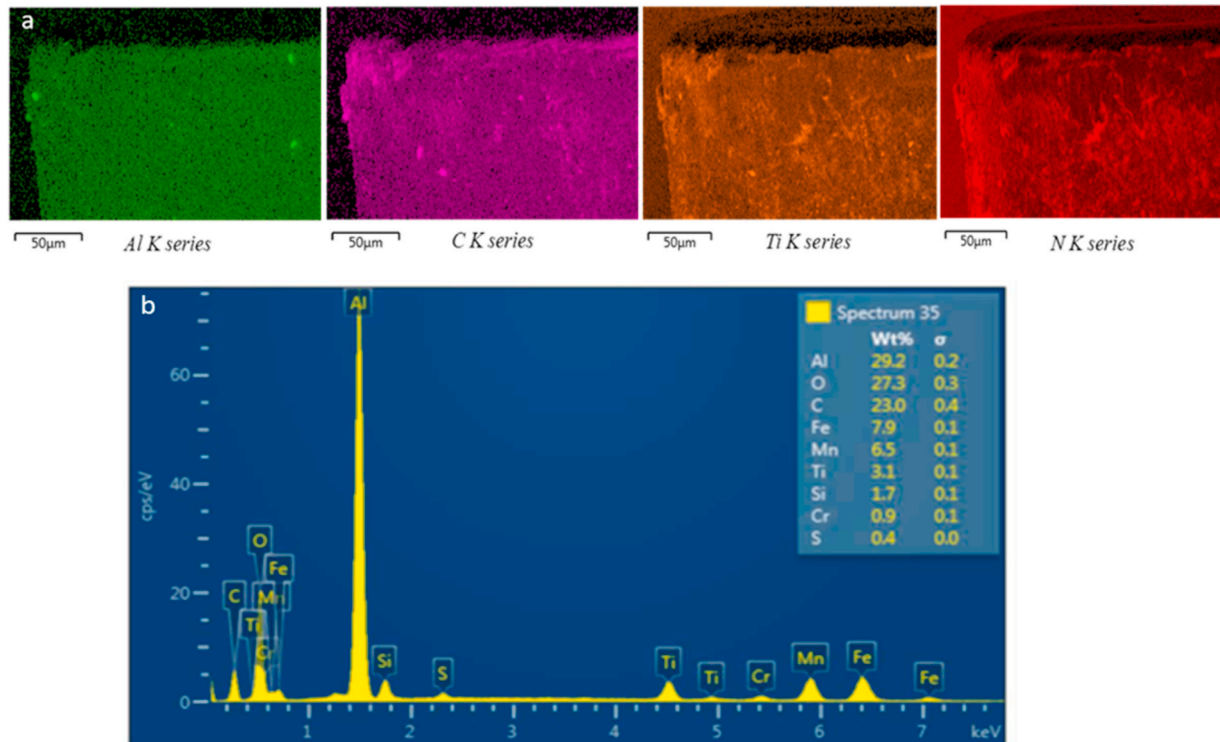


Fig. 9. (a) Elemental mapping of the coating cross-section, showing the spatial distribution of key elements. (b) EDS spectrum on the flank face after 4.5 s of cutting, indicating a high aluminium peak.

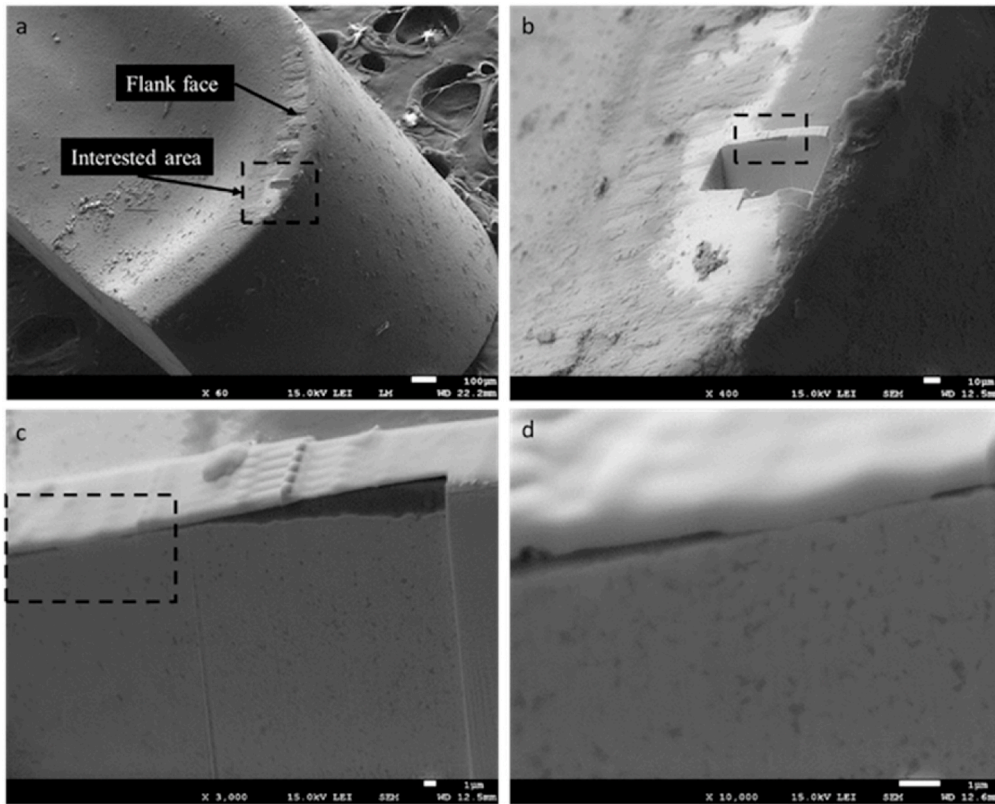


Fig. 10. FIB sequence of the worn flank face after 4.5 s of machining: (a) overall view and (b-d) magnified observations of a selected region, highlighting surface wear, defects, and microstructural features.

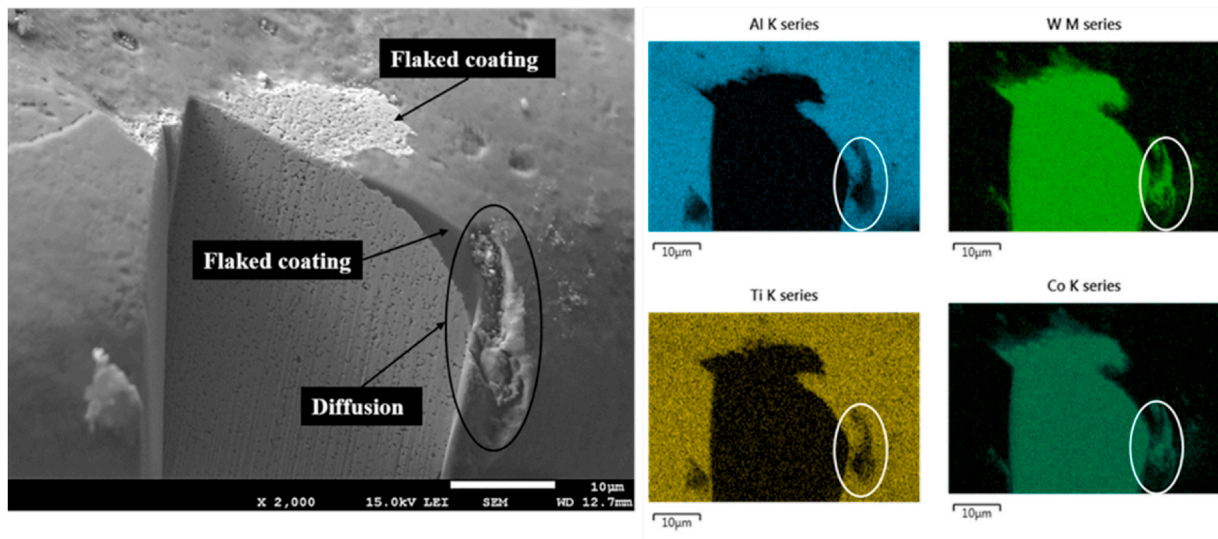


Fig. 11. EDS elemental mapping composition of cobalt diffusing on the flank face of the insert in 4.5 s, as shown in the circled area.

location. The results illustrate diffusion in the worn area after 6.5 s of machining.

After prolonged machining durations, a detailed examination of the coating layer was conducted to assess its protective capabilities, as shown in Figs. 12 and 13. Initial signs of wear, particularly adhesions on the cutting edge, were observed after 4.5 s of machining. As machining continued, the condition of the cutting edge worsened, as evidenced by the flaking of the inner coating and the wear of the outer insert coating. Previous research [15,27,28] has reported the formation of Al-O and Co-O compounds, which can act as protective tribofilms and thermal

barriers at the first transition zone, where initial tool wear ends and steady-state wear begins.

In Fig. 13, the XPS results do not confirm the presence of oxygen; however, diffusion elements such as cobalt (Co) and tungsten (W) from the substrate were detected within the coating. The early presence of these diffusion elements during machining can undermine coating integrity and contribute to subsequent flaking.

Previous research has shown that at elevated temperatures, titanium can chemically react with gases such as oxygen in the air and with elements like carbon. When titanium reacts with carbon, it forms hard

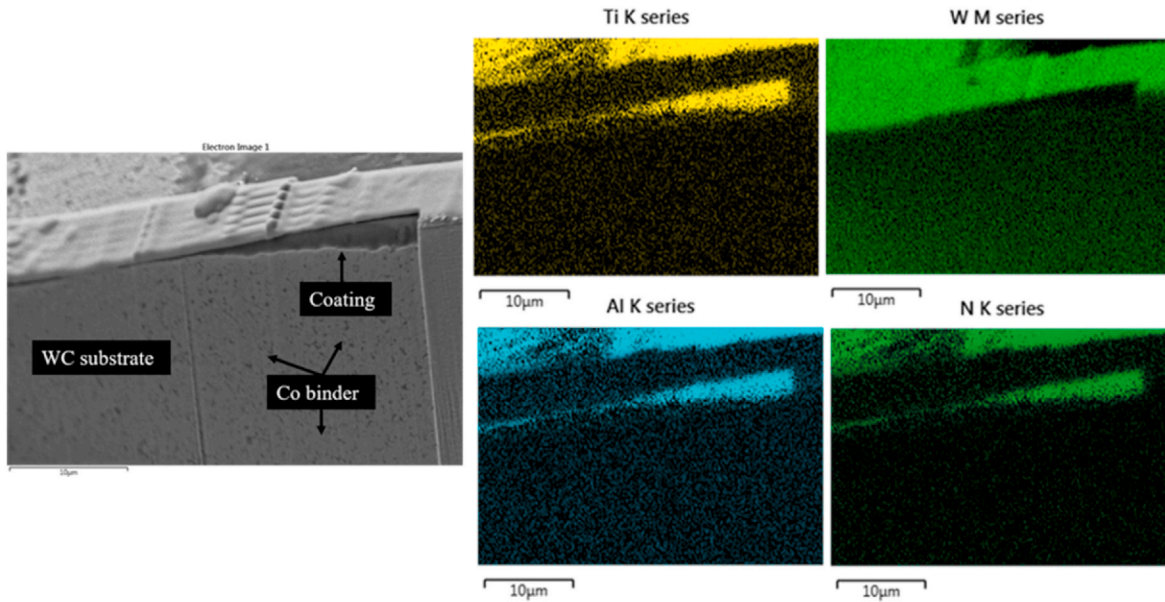


Fig. 12. SEM micrograph and EDS elemental mapping composition at 4.5 s showing aluminium and titanium on the flank face of the insert.

compounds that adhere to the surface. This process starts with the diffusion of carbon from the tool to the workpiece, followed by an interaction between titanium atoms and carbon, leading to the formation of a titanium carbide (TiC) layer [29]. Although the formation of TiC could not be conclusively confirmed, the potential formation of a protective layer might explain the reduced wear rate observed in Fig. 13 between the first and second transition zones.

4. Analysis and discussion

The primary objective of this study was to investigate initial tool wear and to establish a correlation between early wear indicators and subsequent tool failure during the machining of TiMMC. Previous work [17] demonstrated that TiC particles primarily contribute to abrasive wear. Consequently, an increase in the volume fraction of TiC would be expected to shift the dominant wear mechanism toward more severe abrasion. These particles are significantly harder than the cutting tool material and contribute to severe wear. Similar trends have been reported in aluminum matrix composites (AlMMCs), where increasing the content or altering the morphology of hard particles such as SiC resulted in intensified abrasive interactions and reduced tool life [18].

This study focused on initial tool wear and how the wear mechanism in TiMMC machining involves several stages, characterized by a combination of:

- 1 **Spontaneous flaking on coatings:** refers to the accidental separation or peeling of a coating layer from its substrate without any external influence or damage. This issue typically arises due to internal stress within the coating, poor bonding with the substrate, or environmental factors such as temperature fluctuations, humidity, or chemical exposure
- 2 **Edge flaking wear:** Detachment of the protective coating on the tool edge due to high mechanical stress, often resulting from spontaneous flaking.
- 3 **Cohesive flaking wear:** The coating detaches due to the adhering workpiece material, leading to the removal of the underlying substrate during the process
- 4 **Adhesive Wear:** Material from the workpiece adheres to the tool, causing material transfer and wear.
- 5 **Diffusion wear:** Atoms migrate between the tool and workpiece, leading to wear.

6 **Deep cracking:** High thermal and mechanical stresses cause deep cracks to form in the coating and substrate.

7 **Chipping:** Repeated stress cycles lead to small pieces of the tool material chipping off, eventually causing tool failure, often as a result of deep chocking.

Previous research by the authors [15] indicates that various wear mechanisms are active from the beginning of machining until a protective wear layer forms under high stresses and temperatures. Initially, the outer coating layer quickly flakes and peels off, leading to the appearance of cavities on the worn area, which indicates coating removal. These cavities promote diffusion and the formation of micro-cracks, ultimately weakening the tool structure.

Energy-dispersive X-ray spectroscopy (EDS) analysis conducted in the initial seconds of machining showed changes in the elemental composition. At approximately 4.5 s, a high aluminum concentration was detected in the worn area. Aluminum can react with atmospheric oxygen to form aluminum oxide (Al_2O_3), which could contribute to the formation of a protective tribofilm. This tribofilm acts as a protective barrier that minimizes additional wear and safeguards the underlying material of the tool. Al_2O_3 is recognized for its outstanding high-temperature characteristics and has the potential to inhibit further wear due to its thermal stability [28]. Nevertheless, this study did not confirm the formation of Al_2O_3 , as thorough analysis revealed no definitive evidence of its presence.

The hard TiC particles in the workpiece material can abrade the insert surface under mechanical loading, resulting in scratches and grooves on the tool surface. As the coating wears away and delaminates, the substrate becomes exposed, leading to increased adherence of the workpiece material to the substrate, which intensifies adhesive wear, as shown in Fig. 8. Over time, the removal of the coating through wear and delamination further exposes the substrate, leading to even more adherence of the workpiece material to the substrate.

Furthermore, the increase in temperature at the tool–chip interface during machining promotes diffusion, particularly as higher temperatures and strong chemical affinity between titanium and the cutting tool material activate diffusion [29]. This diffusion dissolves some of the substrate, leading to deeper subsurface cracks. Over repeated cycles, these cracks propagate and expand, leading to chipping and ultimately resulting in tool failure [30,31].

Understanding these wear mechanisms is essential for developing

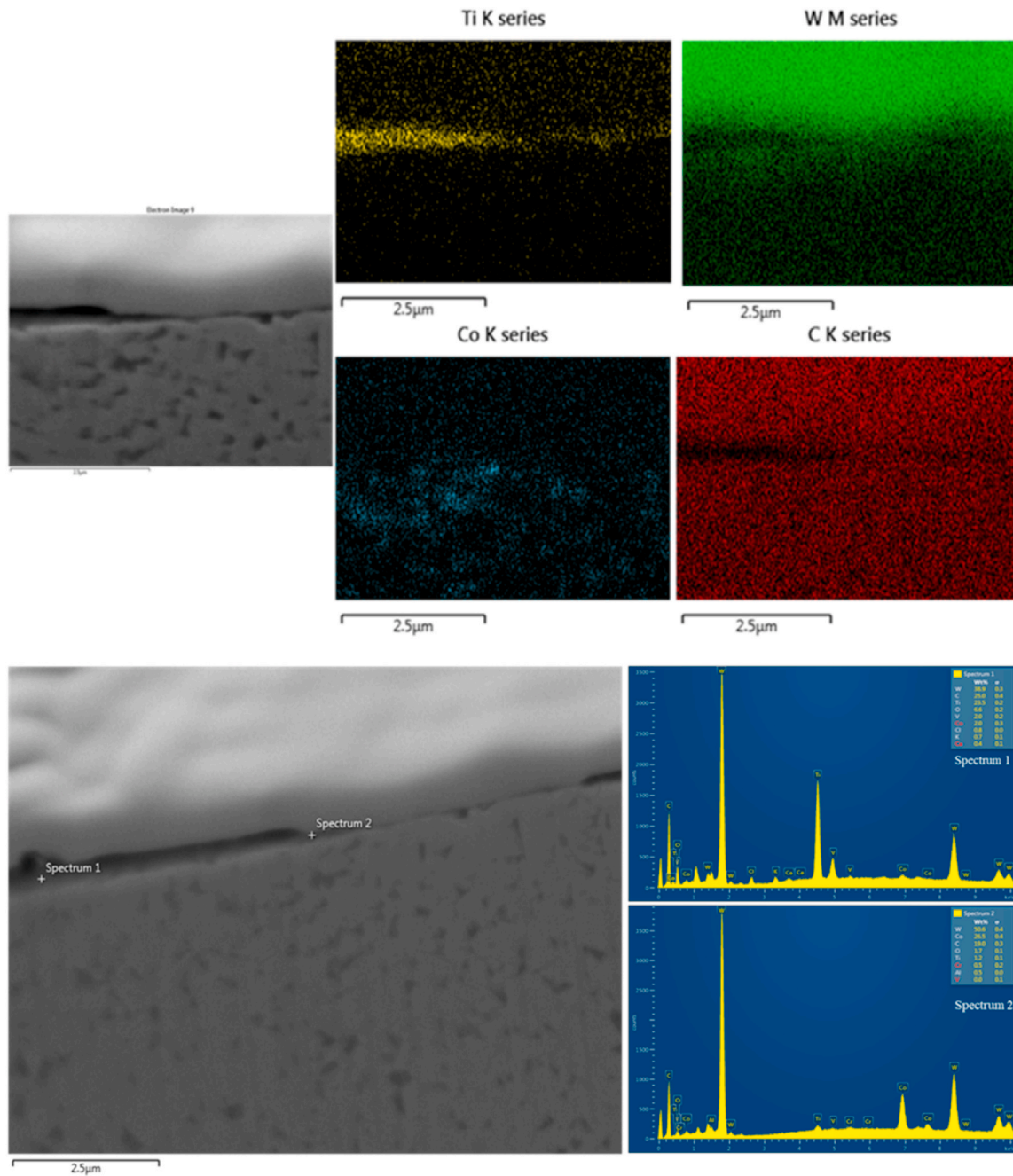


Fig. 13. (a) SEM image and EDS elemental mapping at high magnification. (b) EDS analysis showing tungsten and cobalt concentrations in the dark region.

more wear-resistant tools and optimizing machining parameters to enhance tool life and machining efficiency in TiMMC applications.

Besides its scientific contributions, this study offers significant implications for industry. Many sectors replace cutting tools at the end of their lifespan without fully comprehending the causes of tool wear. Often, the tools are excessively worn, resulting in diminished performance, unanticipated downtime, and increased production costs. The techniques discussed in this paper facilitate predictive maintenance strategies, enabling industries to schedule tool replacements based on real wear patterns rather than arbitrary lifespan estimates. From an industrial application perspective, the findings indicate that the early detection of initial wear signs, such as microcracks and localized flaking, could be used for better accurate predictions of tool life.

This supports the integration of signal-based monitoring techniques—like fractal analysis of cutting forces—into industrial machining

systems. In our case, the results highlight the necessity for coatings with improved adhesion, particularly at the tool edge, especially when machining particle-reinforced composites with uneven dispersion.

5. Conclusions

This study investigates the initial tool wear mechanisms during machining of TiMMC, using SEM, EDS and FIB and analyzing how initial wear can affect directly the final tool wear and failure. By identifying different initial wear mechanism as flaking, adhesion, diffusion, and cracking observations show how the wear evolves into a different type of wear leading eventually to a final tool failure. This work highlights a sequential progression of wear types from initial to final stages, providing valuable insights to improve tool life, optimize machining processes, and enhance production efficiency.

- 1 The study identified various wear mechanisms during the turning of TiMMC, including abrasion, scratching, grooving, smearing, and cracking on the flank face of the cutting tool. Abrasive wear, primarily driven by hard TiC particles embedded in the TiMMC structure, is a significant contributor to wear on the surface of the tool.
- 2 In the initial wear stage, during the first few seconds of machining, mechanisms such as coating flaking, diffusion, and microcracking occur. These early indicators are critical as they set the stage for further wear progression. The initial interaction between the tool and the TiMMC led to the detachment of the protective coatings and the formation of micro-cracks. This weakens the tool surface and makes it more susceptible to further damage as machining continues.
- 3 As machining progresses, wear mechanisms evolve from initial stages like coating flaking to more severe forms by 35 s, including significant chipping and deep cracking. High temperatures and mechanical stresses during machining facilitate the diffusion of elements such as carbon and cobalt, intensifying the wear process. This progression from minor wear to severe material degradation highlights the cumulative and accelerating nature of wear over time.
- 4 Diffusion plays a critical role in wear mechanisms during TiMMC machining. Due to the high chemical affinity between titanium and tool materials, combined with elevated temperatures, elements from the tool diffuse into the workpiece. This diffusion weakens the substrate of the tool, leading to the development of deeper subsurface cracks. Over time, these cracks propagate, ultimately resulting in tool failure.
- 5 From a practical standpoint, the findings suggest that early detection of initial wear indicators such as microcracks and localized flaking could be used to predict tool life more accurately. This supports the integration of signal-based monitoring (e.g., fractal analysis of cutting forces) into industrial machining systems. Additionally, these results underline the need for coatings with enhanced adhesion and thermal resistance, particularly for machining particle-reinforced composites with non-uniform dispersion.
- 6 This study underscores the critical connection between the initial and final wear stages. Early wear phenomena such as coating peeling and minor diffusion gradually evolve into severe wear forms such as chipping and deep cracking. This progression highlights the importance of effectively managing initial wear to delay the onset of more severe mechanisms. Implementing strategies to control early wear is essential for extending tool life and preventing premature tool failure.

Recommendations for future work: To improve tool performance and extend its lifespan in TiMMC machining, optimizing cutting parameters and tool materials is recommended. Techniques such as controlling deposition parameters to minimize residual stress in coatings can be implemented. The use of minimum quantity lubrication (MQL) can help reduce friction and temperature; therefore, reducing the temperature related wear. Future research should prioritize the development of coatings with better thermal stability and adhesion properties to endure the challenging conditions of TiMMC machining.

CRedit authorship contribution statement

M. Marousi: Writing – original draft. **R. Bejjani:** Writing – review & editing, Conceptualization. **M. Balazinski:** Supervision, Conceptualization.

Funding

This research did not receive any specific grant from funding agencies in the public, commercial, or not-for-profit sectors.

Declaration of competing interest

The authors declare that they have no known competing financial interests or personal relationships that could have appeared to influence the work reported in this paper.

Acknowledgments

The authors acknowledge the financial support of the Natural Sciences and Engineering Research Council of Canada (NSERC) and Canadian Network for Research and Innovation in Machining Technology (CANRIMT).

Data availability

Data will be made available on request.

References

- [1] R. Bejjani, et al., Laser assisted turning of titanium metal matrix composite, *CIRP Annals* 60 (1) (2011) 61–64.
- [2] A.K. Srivastava, A.R. Dixit, S. Tiwari, A review on the intensification of metal matrix composites and its nonconventional machining, *Sci. Eng. Compos. Mater.* 25 (2) (2018) 213–228.
- [3] X. Rimpault, M. Balazinski, J.-F. Chatelain, Fractal analysis application outlook for improving process monitoring and machine maintenance in manufacturing 4.0, *J. Manuf. Mater. Processing* 2 (3) (2018) 62.
- [4] H.G. Prengel, State of the art in hard coatings for carbide cutting tools, *Surf. Coating. Technol.* 102 (3) (21 April 1998) 183–190.
- [5] M.D. Hayat, et al., Titanium metal matrix composites: an overview, *Compos. Appl. Sci. Manuf.* 121 (2019) 418–438.
- [6] M. Aramesh, et al., Survival life analysis applied to tool life estimation with variable cutting conditions when machining titanium metal matrix composites (TiMMCs), *Mach. Sci. Technol.* 20 (1) (2016) 132–147.
- [7] B.M. Kramer, On tool materials for high speed, *J. Manuf. Sci. Eng.* 109 (2) (1987. May 1987) 87–91.
- [8] ISO 3685:1993 and ISO 8688-2, 1989.
- [9] X. Duong, J.R.R. Mayer, M. Balazinski, Initial tool wear behavior during machining of titanium metal matrix composite (TiMMCs), *Int. J. Refract. Metals Hard Mater.* 60 (2016) 169–176.
- [10] R. Bejjani, *Machinability and Chip Formation of Titanium Metal Matrix Composites*, 2014.
- [11] J. Paulo Davim, A. Portugal, *Machining Fundamentals and Recent Advances*, Springer, New York Heidelberg Dordrecht London, 2008.
- [12] R. Bejjani, et al., Chip formation and microstructure evolution in the adiabatic shear band when machining titanium metal matrix composites, *Int. J. Mach. Tool Manufact.* 109 (2016) 137–146.
- [13] R. Bejjani, et al., Multi-scale study of initial tool wear on textured alumina coating, and the effect of inclusions in low-alloyed steel, *Tribol. Int.* 100 (2016) 204–212.
- [14] S. Kamalizadeh, et al., Tool wear characterization in high-speed milling of titanium metal matrix composites, *Int. J. Adv. Des. Manuf. Technol.* 100 (9–12) (2018) 2901–2913.
- [15] M. Marousi, et al., Initial tool wear and process monitoring during titanium metal matrix composite machining (TiMMC), *J. Manuf. Process.* 86 (2023) 208–220.
- [16] X. Rimpault, et al., Tool wear and surface quality assessment of CFRP trimming using fractal analyses of the cutting force signals, *CIRP J. Manuf. Sci. Technol.* 16 (2017) 72–80.
- [17] R.B.M. Bejjani, H. Attia, P. Plamondon, G. L'Espérance, Chip formation and microstructure evolution in the adiabatic shear band when machining titanium metal matrix composites, *Int. J. Mach. Tool Manufact.* 109 (2016) 26–35.
- [18] R.R.T. Narayanasamy, R. Karthikeyan, Effect of particulate reinforcement on the mechanical behaviour of sintered Al6061-SiC composites, *Mater. Des.* 30 (2009) 2751–2757.
- [19] J. Yuan, et al., Tribo-films control in adaptive TiAlCrSiYN/TiAlCrN multilayer PVD coating by accelerating the initial machining conditions, *Surf. Coating. Technol.* 294 (2016) 54–61.
- [20] B. Breidenstein, B. Denkena, Significance of residual stress in PVD-coated carbide cutting tools, *CIRP Annals* 62 (1) (2013) 67–70.
- [21] O. Gonzalo, et al., Influence of the coating residual stresses on the tool wear, *Procedia Eng.* 19 (2011) 106–111.
- [22] H. Jia, et al., Stress relaxation related to spontaneous thin film buckling: correlation between finite element calculations and micro diffraction analysis, *Quantum Beam Sci.* 3 (1) (2018) 1.
- [23] I. Dahan, U. A. N. Frage, J. Sariel, M.P. Dariel, Diffusion in Ti/TiC Multilayer Coatings.
- [24] L. Rogström, et al., Structural changes in Ti1-xAlxN coatings during turning: a XANES and EXAFS study of worn tools, *Appl. Surf. Sci.* 612 (2023) 155907.
- [25] G. Fox-Rabinovich, et al., Control of self-organized criticality through adaptive behavior of nano-structured thin film coatings, *Entropy* 18 (8) (2016) 290.
- [26] Stachowiak, G.W., *WEAR, Material, Mechanisms and Practice.* .

- [27] A.M. Khan, et al., Formation of wear-protective tribofilms on different steel surfaces during lubricated sliding, *Tribol. Lett.* 71 (2) (2023).
- [28] J. Yuan, et al., Influence of workpiece material on tool wear performance and tribofilm formation in machining hardened steel, *Lubricants* 4 (2) (2016) 10.
- [29] K. Yang, et al., Formation mechanism of titanium and niobium carbides in hardfacing alloy, *Rare Met.* 36 (8) (2016) 640–644.
- [30] J.F. Luiz, H. Spikes, Tribofilm Formation, friction and wear-reducing properties of some phosphorus-containing antiwear additives, *Tribol. Lett.* 68 (3) (2020).
- [31] Kitagawa, T., Maekawa, K., & Shirakashi, T, Temperature and Wear of Cutting Tools in High-Speed Machining of Inconel 718 and Ti-6Al-6V-2Sn.